ELSEVIER

Polymer 41 (2000) 2203–2212

polymer

Diffusion of acetonitrile in conformational isomers of an H_{12}MDI polyurethane

Y.A. Elabd[a], J.M. Sloan[b], T.A. Barbari[c,*]

[a]*Department of Chemical Engineering, The Johns Hopkins University, Baltimore, MD 21218, USA*
[b]*U.S. Army Research Laboratory, Aberdeen Proving Ground, Aberdeen, MD 21005, USA*
[c]*Department of Chemical Engineering, University of Maryland, College Park, MD 20742, USA*

Received 29 January 1999; received in revised form 1 June 1999; accepted 1 June 1999

Abstract

The diffusion of acetonitrile in conformational isomers of the aliphatic polyurethane, H_{12}MDI (4,4′-dicyclohexylmethane diisocyanate)/BD (1,4-butanediol)/PTMO (poly(tetramethylene oxide)), was investigated at a fixed hard segment content of 29.9 wt%. The effective diffusion coefficient, measured experimentally using FTIR-ATR (Fourier transform infrared-attenuated total reflectance) spectroscopy, decreased as the trans–trans percentage in the hard segment increased. The spectra for the polyurethanes revealed higher fractions of hydrogen-bound C=O (carbonyl) groups at higher trans–trans percentages, which was consistent with higher values of hard segment T_g. During acetonitrile diffusion experiments, a shift from hydrogen-bound to free carbonyl groups in the hard segment domains occurred and hydrogen-bound C≡N and NH peaks appeared suggesting that acetonitrile is solvating to the hard segments in the polymer. Based on these findings, the trend observed for the effective diffusion coefficient may be attributed to tortuosity and penetrant solvation in the polyurethane.

Keywords: Polyurethane; H_{12}MDI; Isomers

1. Introduction

1.1. Polyurethane structure

Polyurethanes are used as coatings, adhesives, thermal insulation and more recently, biomaterials. Thermoplastic polyurethane elastomers are typically phase segregated and consist of a combination of hard, rigid, glassy segments and soft, flexible, rubbery segments. Typically, the hard segments contain a diisocyanate group with a chain extender, a diol or diamine, and the soft segment is usually either a polyether or polyester. Their structure and morphology have been studied extensively [1–7] because of their excellent elastomeric and thermal properties.

1.2. Phase segregation

The elastomeric properties of polyurethanes can be attributed to phase segregation. Many studies [2,4,5,8] have shown that microphase segregation occurs in polyurethanes due to the thermodynamic incompatibility of the hard and soft segments and physical crosslinking among hard segments. Phase segregation leads to a variety of morphologies depending on the content of hard or soft segment in the polymer. Usually, at phase ratios greater than 2:1, the minority phase is dispersed in a matrix of the majority phase, while at near 1:1 phase ratios, lamellae structures are observed [7,12]. The extent of segregation varies depending on the amount of physical crosslinking that takes place, usually through hydrogen bonding. Hydrogen bonding can occur between the urethane groups of different hard segments, or between the urethane group in a hard segment and the oxygen in a polyether or polyester soft segment [8,23,25]. More crosslinking between hard segments leads to a higher degree of phase segregation while hydrogen bonding between hard and soft segments leads to phase mixing.

1.3. H_{12}MDI

Polyurethane hard segments consist of a diisocyanate group, which can contain either aromatic rings, usually MDI (4,4′-diphenylmethane diisocyanate) or TDI (2,4-toluene diisocyanate), or aliphatic rings such as H_{12}MDI (4,4′-dicyclohexylmethane diisocyanate). Both aromatic and aliphatic hard segments have been studied [1–8,27,28]

* Corresponding author. Tel.: +1-301-405-2983; fax: +1-301-405-0523.
E-mail address: barbari@eng.umd.edu (T.A. Barbari)

0032-3861/00/$ - see front matter
PII: S0032-3861(99)00398-5

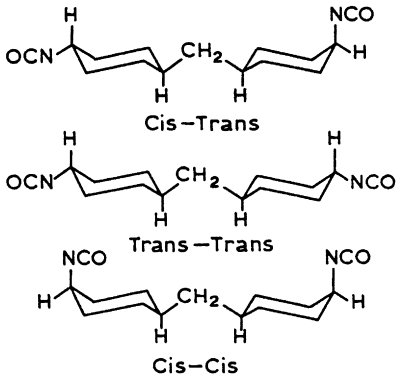

Fig. 1. H_{12}MDI conformational isomers.

and one difference to note between the two is the ability of the latter to isomerize. Byrne et al. [9] have studied the properties of the conformational isomers of H_{12}MDI polyurethanes and have shown that H_{12}MDI can exist as three separate isomers, cis–cis, cis–trans, and trans–trans (Fig. 1).

1.4. FTIR-ATR

Several investigators have studied small molecule diffusion through polyurethanes using such techniques as mass spectroscopy and gravimetric sorption [10–17]. In this study, FTIR-ATR (Fourier transform infrared-attenuated total reflectance) spectroscopy [18–21] was used to measure the effective diffusion coefficients of acetonitrile in aliphatic polyurethane films. Hong et al. [20] compared this technique with conventional gravimetric sorption to confirm its accuracy. This technique can examine multicomponent penetrant diffusion [21], characteristics of the polymer during diffusion, and penetrant interactions with the polymer.

1.5. Objective

Although many papers have documented structure–property relationships [1–8] of polyurethane elastomers and the effect of varying hard segment content on small molecule diffusion [10–17], few have investigated the effect of varying isomer content on polymer properties [9,27,28]. In this paper, the effect of varying isomer content at a fixed hard segment content on the diffusion of acetonitrile was examined with FTIR-ATR spectroscopy and thermal analysis.

Table 1
H_{12}MDI/BD/PTMO 2000 conformational isomer samples

Sample	Cis–cis (%)	Cis–trans (%)	Trans–trans (%)
H_{12}MDI-90	1	9	90
H_{12}MDI-64	5	31	64
H_{12}MDI-53	7	40	53
H_{12}MDI-29	10	61	29

2. Experimental

2.1. Materials and sample preparation

Samples of H_{12}MDI/BD/PTMO 2000 polyurethane were supplied and synthesized by the Army Materials and Mechanics Research Center [9]. H_{12}MDI (4,4′-dicyclohexylmethane diisocyanate) is the hard segment, BD (1,4-butanediol) is a chain extender, and PTMO 2000 (poly(tetramethylene oxide)) (mol. wt. 2000) is the polyether soft segment. The polyurethanes were synthesized by separating H_{12}MDI hard segment isomers by fractional crystallization and adding PTMO 2000 to form a prepolymer. The prepolymer was then cured with the 1,4-butanediol at a constant hard segment content of 29.9 wt%. The diisocyanate isomer contents of the polyurethanes used in these experiments are shown in Table 1. Acetonitrile, hexane, and polyether glycol 650 (Terathane®) (mol. wt. 650) were obtained from Aldrich.

Samples for the FTIR-ATR experiments were prepared by pipetting a 5 wt% solution of each H_{12}MDI/BD/PTMO 2000 sample in chloroform on a level ATR crystal. After drying for 24 h in a clean hood, the films were placed in a vacuum oven to remove residual solvent for approximately 24 h at 50°C. No residual chloroform was detected spectroscopically in the film attached to the ATR crystal, confirming solvent removal.

2.2. ATR diffusion experiments

An FTIR spectrometer (Mattson Research Series 1®) with a horizontal ATR cell (Fig. 2) and a zinc selenide trapezoidal ATR crystal (Graseby Specac) was used to obtain all infrared spectra for the diffusion experiments. The ATR crystal had entry and exit beveled faces at a 45° angle of incidence for the IR beam and a refractive index of 2.4. The liquid penetrant is injected into the top of the cell and the ATR cell can be temperature regulated by circulating water from a bath through the outside jacket of the cell. In this study, the diffusion experiments were conducted at room temperature, 23 ± 1°C. The sampling parameters for the FTIR-ATR experiments are provided in Table 2. Film thickness, which ranged from 60 to 90 microns for the spectroscopic experiments, was measured using a micrometer [20–21].

2.3. Diffusion model

The one-dimensional continuity equation for a single penetrant was used to model these experiments with a concentration-averaged effective diffusion coefficient taken as constant.

$$\frac{\partial C}{\partial t} = D_{\text{eff}} \frac{\partial^2 C}{\partial x^2} \tag{1}$$

In Eq. (1), C is the concentration of the penetrant and D_{eff} is the effective diffusion coefficient. Referring to Fig. 2, the

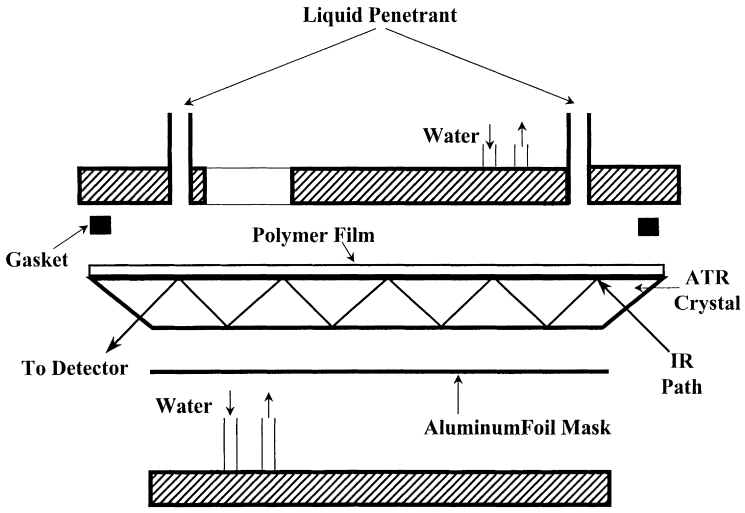

Fig. 2. Schematic of the ATR cell.

surface exposed to the penetrant corresponds to $x = L$ in the model while that attached to the ATR crystal corresponds to $x = 0$. The initial and boundary conditions for a polymer film of thickness L exposed to an infinite reservoir of penetrant are:

$$C = 0 \qquad \text{at} \qquad 0 < x < L, \;\; t = 0 \tag{2}$$

$$\frac{\partial C}{\partial x} = 0 \qquad \text{at} \qquad x = 0, \;\; t \geq 0 \tag{3}$$

$$C = C_L \qquad \text{at} \qquad x = L, \;\; t \geq 0 \tag{4}$$

The Laplace solution to Eq. (1) with these boundary and initial conditions is

$$\frac{C}{C_L} = 1 - \frac{4}{\pi}\sum_{n=0}^{\infty}\frac{(-1)^n}{2n+1} \times \exp\left[\frac{-D(2n+1)^2\pi^2 t}{4L^2}\right]\cos\left[\frac{(2n+1)\pi x}{2L}\right] \tag{5}$$

Eq. (5) can be related to the experimental infrared absorbance data with the use of the ATR differential form of the Beer–Lambert law [18–21]

$$A = \int_0^L \epsilon^* C E_0^2 \exp\left(\frac{-2z}{d_p}\right) \mathrm{d}z \tag{6}$$

where ϵ^* is an effective extinction coefficient for FTIR-ATR spectroscopy, A the ATR absorbance, E_0 the field strength at $z = 0$, and d_p is the depth of penetration for the IR beam into the polymer film. Substituting Eq. (5) into the absorbance expression, with assumptions of weak infrared absorption and negligible changes in polymer refractive index [18–21], results in

$$\frac{A_t}{A_{eq}} = 1 - \frac{8}{\pi d_p(1 - e^{-2L/d_p})}\sum_{n=0}^{\infty}\frac{e^g[f e^{-2L/d_p} + (-1)^n(2/d_p)]}{(2n+1)(4/d_p^2 + f^2)} \tag{7}$$

where

$$g = \frac{-D(2n+1)^2\pi^2 t}{4L^2} \tag{8}$$

$$f = \frac{(2n+1)\pi}{2L} \tag{9}$$

$$d_p = \frac{\lambda}{2n_2\pi\sqrt{\sin^2\theta - (n_1/n_2)^2}} \tag{10}$$

The effective diffusion coefficient can be determined by regressing the experimental data to Eq. (7), where A_t is the integrated infrared absorbance of the diffusing penetrant at time t, and A_{eq} is its value at equilibrium. The other constants arise from the physics of attenuated total reflectance [18–19] where n_1 and n_2 are the refractive indices of the polymer (1.47) and the ATR crystal (2.4), respectively, θ the angle of incidence, and λ is the wavelength of absorbed light.

Table 2
Sampling parameters used in FTIR-ATR experiments

Parameter	Value
Resolution	4 cm^{-1}
Starting wavenumber	675 cm^{-1}
Ending wavenumber	4000 cm^{-1}
Sample scans	20
Signal gain	1
Scan velocity	2.5 cm/s
Sampling time	6.6 s

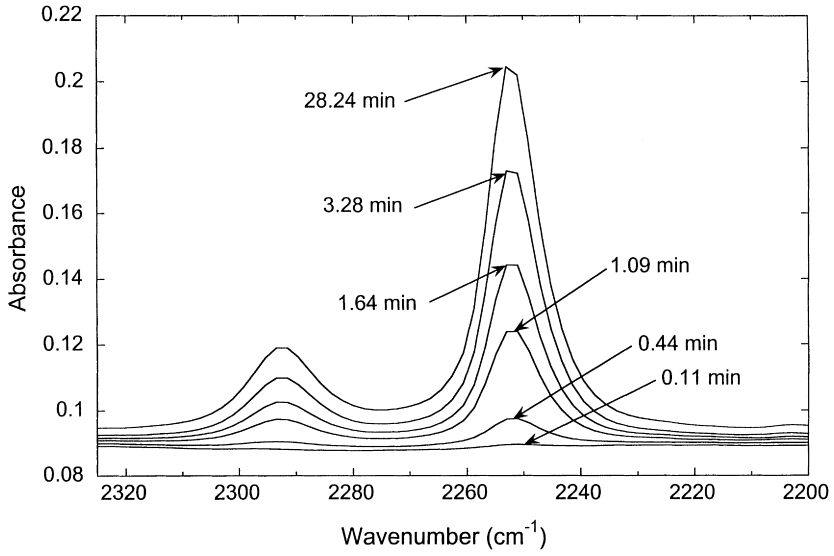

Fig. 3. Time-evolved acetonitrile absorbance spectra in H_{12}MDI/BD/PTMO2000 (64% trans–trans isomer content).

2.4. Thermal analysis experiments

The glass transition temperatures of the hard segments were determined by differential scanning calorimetry (DSC) using the midpoint with a heating rate of 20°C/min and sample weights of 10 ± 1 mg. Dynamic mechanical thermal analysis (DMTA), with a heating rate of 5°C/min and temperature range of -100 to $+100$°C, was used to determine the glass transition temperatures of the soft segments using samples that were $10(\pm 0.6) \times 13(\pm 0.2)$ mm and $1(\pm 0.1)$ mm thick. The loss modulus method was used to determine the glass transition temperatures of the soft segments.

3. Results and discussion

3.1. Diffusion coefficients

Time-evolved spectra for acetonitrile diffusion in one of the polyurethane samples are shown in Fig. 3. Two bands are present over the range shown, 2253 and 2294 cm^{-1}, representing vibration modes of acetonitrile. The larger band at 2253 cm^{-1} is assigned to the C≡N stretching mode and the weaker band at 2294 cm^{-1} is a combination of both CH_3 bending and C–C stretching modes [29,30]. This region was integrated at each time point using a numerical peak integration algorithm in WinFIRST® (Mattson

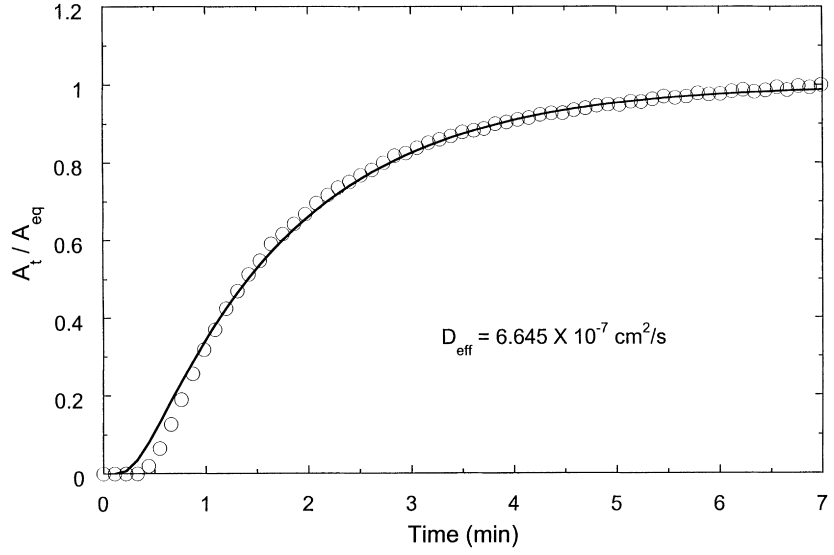

Fig. 4. Acetonitrile diffusion data regressed with Fickian model (64% trans–trans isomer content).

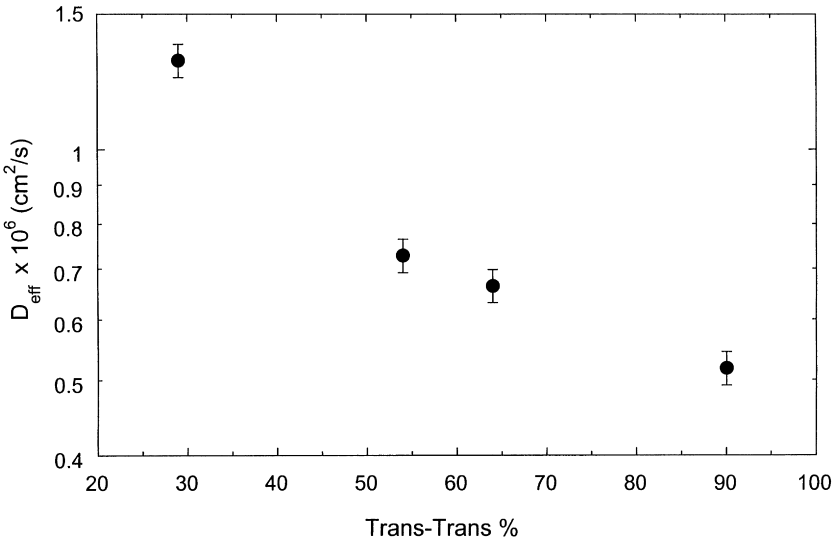

Fig. 5. Effective diffusion coefficients for H_{12}MDI polyurethane isomers.

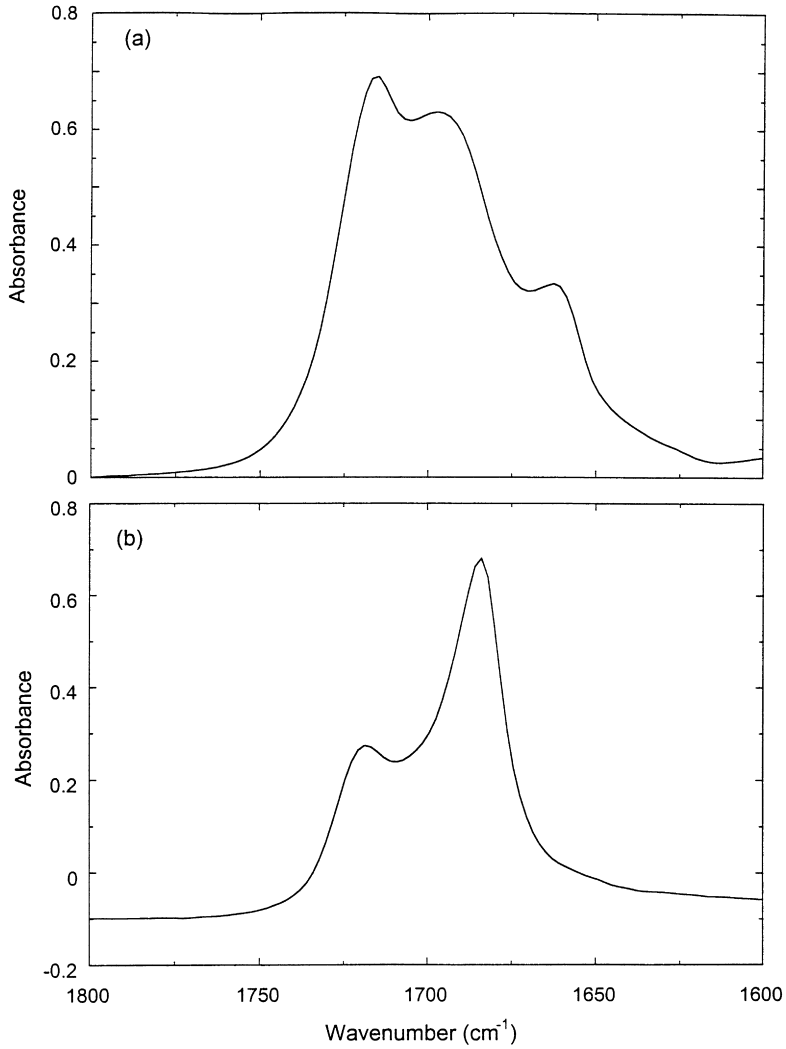

Fig. 6. Carbonyl absorbance spectra for H_{12}MDI hard segment: (a) 29% and (b) 90% trans–trans isomer content.

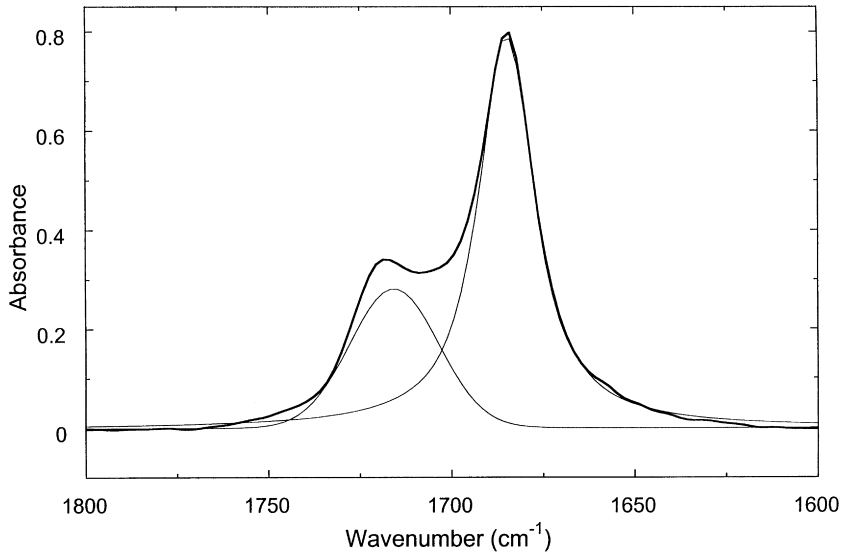

Fig. 7. Deconvolution of a typical carbonyl absorbance spectrum (90% trans–trans isomer content).

Table 3
Changing percentage of free carbonyl population in the polyurethane samples

Sample	Trans–trans (%)	Free carbonyl (%)	
		Without acetonitrile	With acetonitrile[a]
H_{12}MDI-90	90	29	50
H_{12}MDI-64	64	30	36
H_{12}MDI-53	53	46	55
H_{12}MDI-29	29	41	49

[a] At equilibrium sorption.

Instruments) over the wavelength range of 2325–2213 cm^{-1}. The effective diffusion coefficient was then determined by regressing the integrated absorbance data with Eq. (7) using a least squares regression technique [18–21] as shown in Fig. 4 for one of the samples. All of the isomer samples displayed Fickian behavior similar to Fig. 4. Other investigators [10–13] have shown Fickian behavior in polyurethanes at low hard segment contents, while also observing relaxation effects at higher hard segment contents [10,12]. Fig. 5 shows the trend in the effective diffusion coefficient with varying isomer content. The effective diffusion coefficient decreased with increasing trans–trans percentage of the hard segment. The magnitude of the diffusion coefficients measured here is consistent with that for rubbery polymers in general, suggesting diffusion occurs through the soft segment matrix. At this hard segment content, other investigators [10–17] have shown that diffusion occurs in the soft segment matrix in a tortuous path around dispersed hard segment domains.

3.2. Hard segment domains

To aid in understanding the results from Fig. 5, the hard segment C=O (carbonyl) spectra and the glass transition temperatures of the hard and soft segments were examined. The carbonyl stretching region for the 29 and 90% trans–trans samples are shown in Fig. 6. For the 90% trans–trans sample, two peaks are evident, a free carbonyl band at 1720 cm^{-1} and a hydrogen-bound carbonyl band at 1685 cm^{-1}. In the 29% trans–trans sample, three peaks appear, a free carbonyl band at 1720 cm^{-1}, a hydrogen-bound carbonyl band at 1695 cm^{-1}, and an additional band at 1660 cm^{-1} which other investigators have identified as urea linkages within the hard domains [22,24]. The urea band was detected only in the H_{12}MDI-29 and H_{12}MDI-53 samples. To quantitatively analyze the change which occurs with the carbonyl groups of the different isomer samples, the spectra were deconvoluted (Fig. 7) using a peak fitting algorithm in Advanced FIRST® (Mattson Instruments). This algorithm deconvoluted the overlapping peaks by fitting synthetic Gauss–Lorentz sum peaks to the experimental

Table 4
Glass transition temperatures of soft and hard segments in polyurethane samples

Sample	Trans–trans (%)	Soft segment T_g (°C)	Hard segment T_g (°C)
H_{12}MDI-90	90	− 54	178
H_{12}MDI-64	64	− 54	147
H_{12}MDI-53	53	− 54	128
H_{12}MDI-29	29	− 54	128

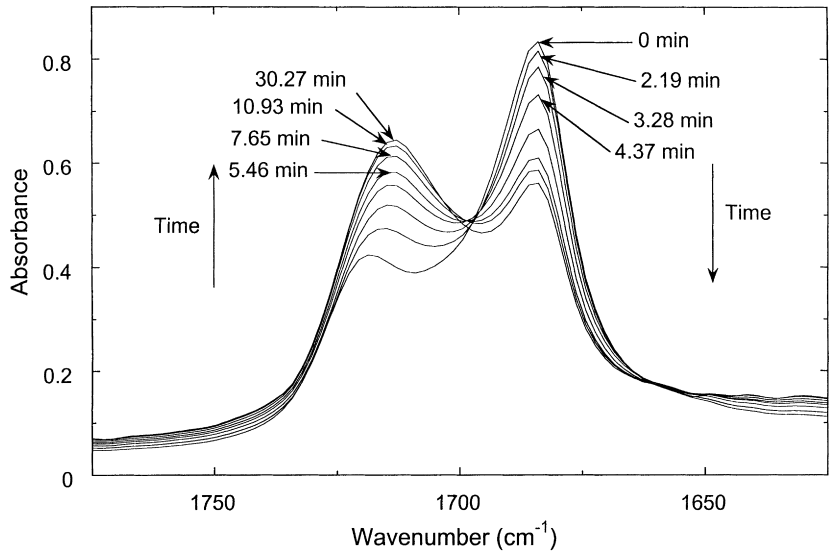

Fig. 8. Time-evolved carbonyl absorbance spectra (90% trans–trans isomer content) during acetonitrile diffusion.

data at each time point to determine the integrated absorbance of the separate bands [19]. To quantify the difference between the two populations of carbonyl groups, the fraction of free carbonyls was determined assuming the same extinction coefficients for both bound and free carbonyl bands [22–26] (the urea band was included with hydrogen-bound urethane carbonyl groups). At higher trans–trans isomer content in the hard segments, the infrared

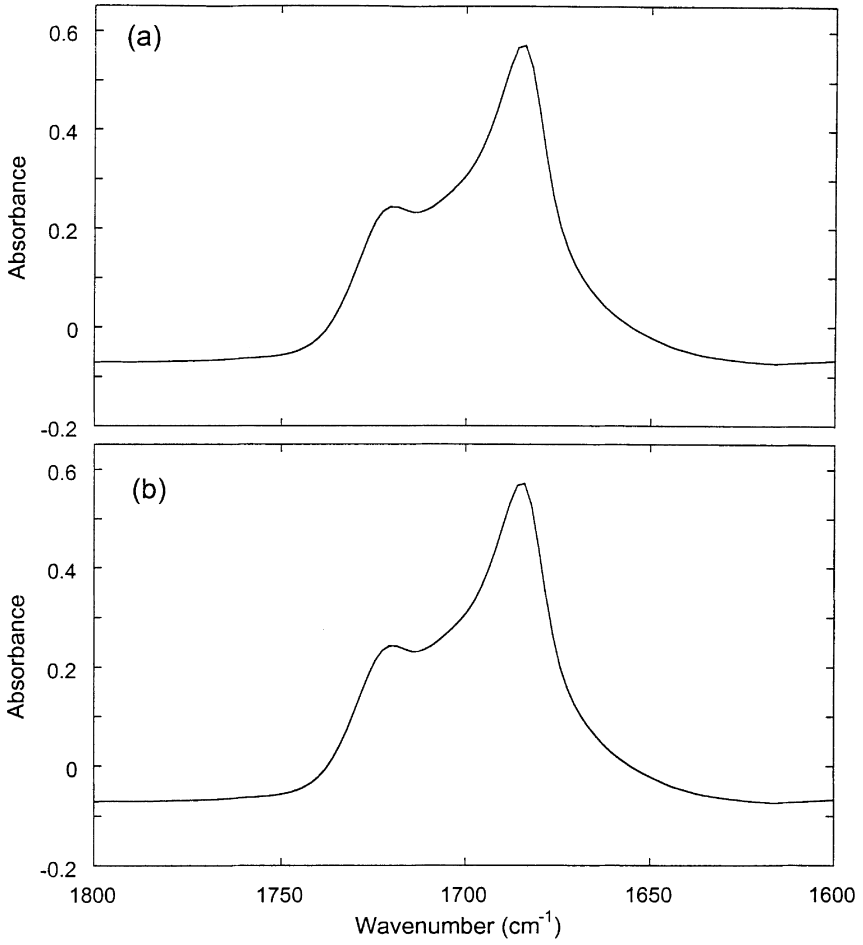

Fig. 9. Carbonyl absorbance spectrum for hexane diffusion (90% trans–trans isomer content): (a) before diffusion experiment; (b) in the presence of hexane.

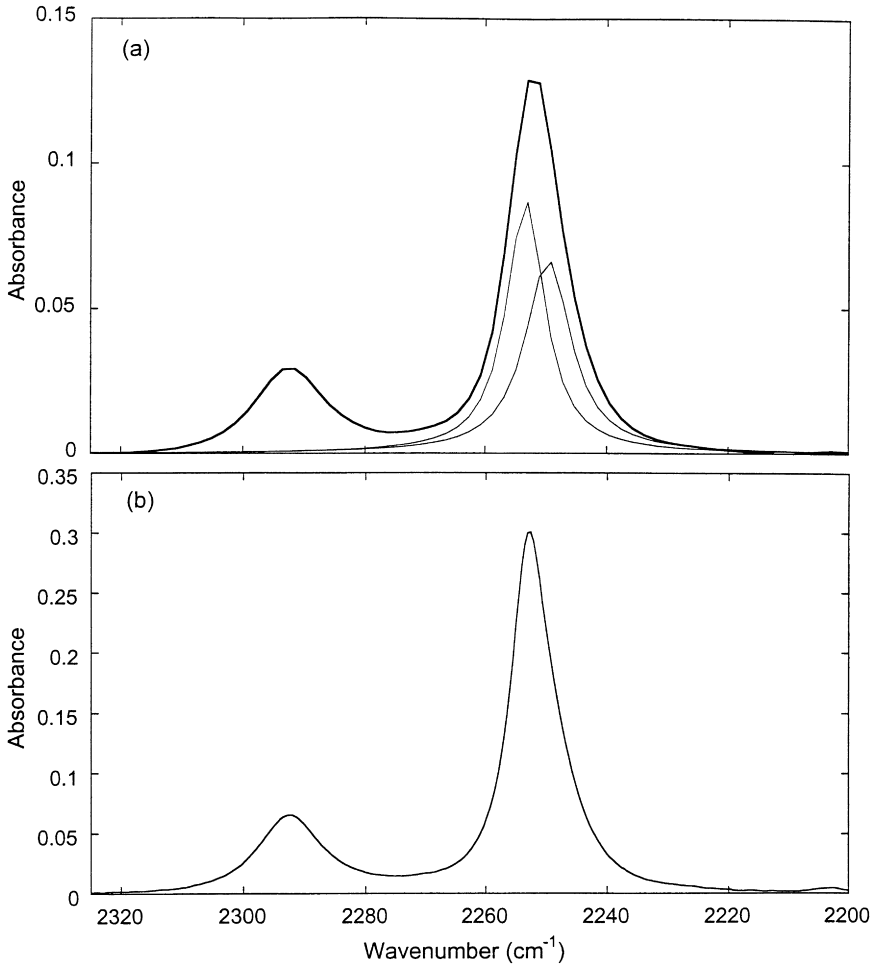

Fig. 10. Deconvolution of C≡N spectrum: (a) in H_{12}MDI polyurethane (90% trans–trans isomer content); (b) in polyether glycol 650.

spectra show higher extents of hydrogen bonding (lower free carbonyl content) consistent with a previous study [9] (see Table 3).

The glass transition temperatures are listed in Table 4. The glass transition temperature of the hard segment increases with increasing trans–trans isomer content among the samples. Physically, more hydrogen bonding among hard segments requires more thermal energy for the glass transition. The glass transition temperature of the soft segments remains constant at −54°C for all isomer samples (Table 4), which indicates no changes in the degree of phase mixing.

Several investigators have shown decreasing diffusion coefficients with an increase in hard segment content, which were explained by a reduction in soft segment mobility because of phase mixing [10,11,15,17] This investigation differs from previous ones because the hard segment content remains constant among the samples, only the isomer content within the hard segment is different. The results here suggest that increasing trans–trans percentage may result in an increase in the number of impermeable hydrogen-bound hard segment domains, which causes the effective diffusion coefficient to decrease owing to increased tortuosity. The greater extent of hydrogen bonding indicates that these domains may be more ordered at higher trans–trans percentages.

3.3. Acetonitrile solvation to hard segments

The carbonyl, C≡N, and NH stretching bands were monitored during the diffusion process to determine if there were any molecular interactions between acetonitrile and the polymer. In Fig. 8, the time-evolved carbonyl spectra are shown for the H_{12}MDI-90 sample. Interestingly, the free carbonyl band (1720 cm^{-1}) increases while the hydrogen-bound carbonyl band (1685 cm^{-1}) decreases during the diffusion experiment (see Table 3). During the diffusion experiments, the urea band remained constant in the H_{12}MDI-29 and H_{12}MDI-53 samples. These observations suggest that acetonitrile either competes with carbonyls for hydrogen bonding to the NH groups and solvates to the hard segments or induces swelling to the extent that hydrogen bonding is disrupted. To determine which of the two mechanisms is responsible, the carbonyl region was

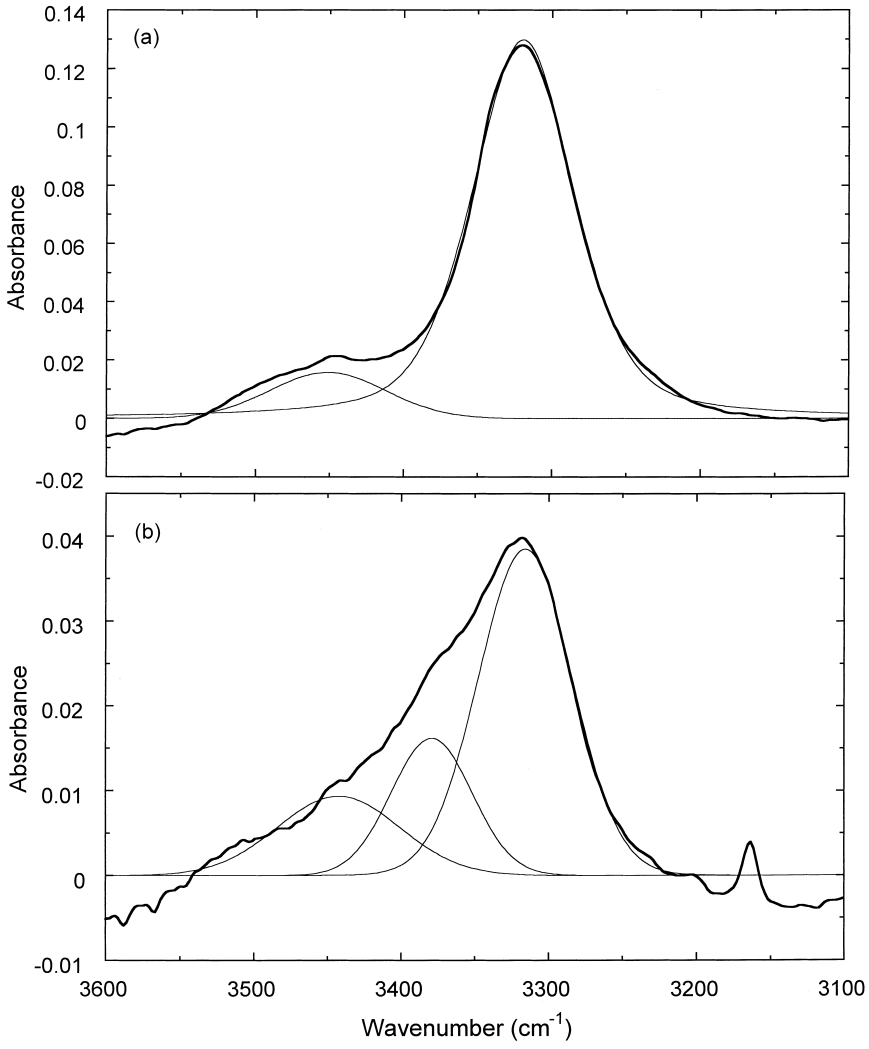

Fig. 11. Deconvolution of NH absorbance spectrum (90% trans–trans isomer content): (a) before diffusion experiment; (b) in the presence of acetonitrile.

examined during a diffusion experiment with hexane, a penetrant with a mass uptake in the polymer comparable to that of acetonitrile (~2 wt%). Fig. 9 shows the carbonyl bands with and without hexane present in the polyurethane. Shifting between carbonyl groups was not observed with hexane, suggesting acetonitrile solvation to the hard segments of the polyurethanes.

Fig. 10 further supports acetonitrile solvation by comparing the C≡N stretching band in the polyurethane (Fig. 10a) with that in a low molecular weight soft segment analog, polyether glycol 650 (Fig. 10b). In Fig. 10a, the C≡N band is deconvoluted at equilibrium sorption showing the free band and the hydrogen-bound band, while Fig. 10b shows no hydrogen-bonding effects in the soft segment alone. The shifting of the C≡N stretch during hydrogen bonding has been observed by other investigators [29,30].

Additionally, NH stretching bands were examined to provide more information about the hydrogen bonding that takes place in the polyurethane. Three proton acceptor groups in polyurethanes can hydrogen bond to the NH group: the carbonyl group in the hard segment, the oxygen of the polyether soft segment, and the alkoxy oxygen in the hard segment [25]. If the amount of hydrogen bonding with the alkoxy oxygen is assumed to be small [25], the peak at 3300 cm^{-1} represents hydrogen bonding of the NH group with both the carbonyl group in other hard segments and with ether oxygens in the soft segments. Deconvolution of the NH band prior to a diffusion experiment is shown in Fig. 11a. The peak located at 3430 cm^{-1} represents free NH groups, and the one at 3300 cm^{-1} represents hydrogen-bound NH groups [22–26]. Fig. 11b displays a decrease in the absorbance intensity because of spectral broadening in the presence of acetonitrile. This occurs because an additional peak at 3380 cm^{-1} appears in the NH region at the conclusion of a diffusion experiment as shown in Fig. 11b. Differences in the extinction coefficient among the NH peaks may also contribute to the decrease in intensity [26]. This additional peak may be the result of hydrogen bonding between the NH group and the acetonitrile, again suggesting solvation of the penetrant to the hard segments.

Since penetrant solvation to a polymer can hinder diffusion, these results suggest that hydrogen bonding between acetonitrile and the polyurethane may influence the trend in the effective diffusion coefficient.

4. Conclusions and future directions

Fickian diffusion behavior was observed among all H_{12}MDI polyurethanes, 29, 53, 64, and 90% trans–trans content, using the FTIR-ATR spectroscopy technique. At a fixed hard segment content of 29.9 wt%, the effective diffusion coefficient decreased with increasing trans–trans percentage. From spectroscopic and thermal analyses, there is evidence of increased hydrogen bonding among hard segments as the trans–trans isomer content increases. Further study of the carbonyl, C≡N, and NH regions of the spectra during the diffusion experiments demonstrate that solvation occurs between acetonitrile and the NH groups on the hard segments of the polyurethane. These results suggest that the value of the effective diffusion coefficient is influenced by tortuosity and penetrant solvation to the hard segments. At present, a diffusion model is under development to account for solvation in a phase-segregated polymer which will be combined with small-angle X-ray scattering experiments to determine the size of the hard segment domains.

Acknowledgements

The authors acknowledge the financial support of the U.S. Army Research Office through the Grant DAAH04-96-1-0133 and the Army Research Laboratory Materials Center of Excellence through Grant DAAH04-96-2-0006.

References

[1] Cooper SL, Tobolsky AVJ. Appl Polym Sci 1966;10:1837.
[2] Bonart R. J Macromol Sci-Phys B 1968;2:115.
[3] Schneider NS, Despar CR, Illinger JL, King AO. J Macromol Sci-Phys B 1975;11:527.
[4] Van Bogart JWC, Lilaonitkul A, Lerner LE, Cooper SL. J Macromol Sci-Phys B 1980;17:267.
[5] Abouzahr S, Wilkes GL, Ophir Z. Polymer 1982;23:1077.
[6] Speckhard TA, Hwang KKS, Cooper SL, Chang VSC, Kennedy JP. Polymer 1985;26:70.
[7] Chen-Tsai CHY, Thomas EL, MacKnight WJ, Schneider NS. Polymer 1986;27:659.
[8] Lagasse RRJ. Appl Polym Sci 1977;21:2489.
[9] Byrne CA, Mack DP, Sloan JM. Rub Chem Technol 1985;58:985.
[10] Goydan R, Schneider NS, Meldon J. Polym Mater Sci Eng 1983;49:249.
[11] McBride JS, Massaro TA, Cooper SL. J Appl Polym Sci 1979;23:201.
[12] Serrano M, MacKnight WJ, Thomas EL, Ottino JM. Polymer 1987;28:1674.
[13] Ziegel KD. J Macromol Sci-Phys B 1971;5:11.
[14] Aithal US, Aminabhavi TM. Polymer 1990;31:1757.
[15] Sreenivasan K. J Macromol Sci-Phys B 1993;32:125.
[16] Sreenivasan K. J Polym Sci Part B 1993;31:1083.
[17] Sreenivasan K. Polymer J 1990;22:620.
[18] Fieldson GT, Barbari TA. Polymer 1993;34:1146.
[19] Fieldson GT, Barbari TA. AIChE J 1995;41:795.
[20] Hong SU, Barbari TA, Sloan JM. J Polym Sci: Polym Phys Ed 1997;35:1261.
[21] Hong SU, Barbari TA, Sloan JM. J Polym Sci: Polym Phys Ed 1998;36:337.
[22] Teo LS, Chen CY, Kuo JF. Macromolecules 1997;30:1793.
[23] Senich GA, MacKnight WJ. Macromolecules 1980;13:106.
[24] Wang CB, Cooper SL. Macromolecules 1983;16:775.
[25] Sung CSP, Schneider NS. J Mater Sci 1978;13:1689.
[26] MacKnight WJ, Yang M. Polym Sci Part C 1973;42:817.
[27] Seneker SD, Born L, Schmelzer HG, Eisenbach CD, Fischer K. Colloid Polym Sci 1992;270:543.
[28] Joseph MD, Savina MR, Harris RF. J Appl Polym Sci 1992;44:1125.
[29] Takamuku T, Tabata M, Yamaguchi A, Nishimoto J, Kumamoto M, Wakita H, Yamaguchi T. J Phys Chem B 1998;102:8880.
[30] Jamroz D, Stangret J, Lingdren J. J Am Chem Soc 1993;115:6165.